KSME Journal, Vol. 7, No. 2, pp. 165~172, 1993

An Experimental Study on Heat Transfer Characteristics for a Horizontal Tubular Array in a High-Temperature Fluidized Bed

Tae-Yong Chung*

(Received November 27, 1992)

Experiments were performed with an array of horizontal tubes, arranged in a regular equilateral triangular pattern, immersed in a fluidized bed. Three different bed operating temperatures were used, these being 705, 761 and 812 K. Data are reported for heat transfer between the bed and a centrally-located tube in the array. Both total and radiative heat transfer rates were measured for three different sizes of particles and for superficial velocities spanning the range from packed bed conditions to over twice the minimum fluidization velocity. Local heat transfer values, measured around the tube periphery, and integrated averages are reported for all test conditions.

Key Words: Total Heat Transfer, Radiative Heat Transfer, High Temperature Fluidized Bed, Tubular Array, Superficial Velocity

Nomenclature

Ar : Archimedes number $[=\frac{gDp^3(\rho_p-\rho_f)\rho_f}{\mu_f{}^2}]$
C_{ps} : Particle specific heat at constant pressure
Dp : Particle diameter
$\overline{Dp}$: Mean particle diameter
Dp_i : Mean open diameter in sieve
g : Gravitational acceleration
h_{max} : Spatial-averaged maximum total heat transfer coefficient
k_f : Gas thermal conductivity
k_p : Particle thermal conductivity
Nu_{max} : Spatial-averaged maximum Nusselt number $[=\frac{h_{max}Dp}{k_f}]$
Umf : Minimum fluidizing velocity
Uo : Superficial velocity
ρ_f : Gas density
ρ_p : Particle density
μ_f : Gas viscosity
ε_p : Particle emissivity
θ : Angle from lower stagnation point, degrees

* Department of Mechanical Engineering Kookmin University, Seoul, 136-702, Korea

1. Introduction

The use of fluidized beds as combustion zones for coal-fired power plants has generated interest in the heat transfer capabilities of these devices. The ability of limestone to adsorb SO_x makes fluidized beds composed of limestone particles attractive from the standpoint of rendering airborne emissions more environmentally acceptable. It happens that the dynamic character of fluidized beds also enhances heat transfer rates between hot beds and immersed surfaces which, in the power plant application, would be arrays of tubes carrying the water-steam working fluid. Improved heat transfer characteristics allow the desired energy transport to occur at lower-than-normal temperatures thereby decreasing No_x emissions also.

A fundamental knowledge of heat transfer in

high-temperature fluidized beds is essential for proper design and optimization of such a combustor. High-temperature heat transfer is significantly difficult to describe since convective and radiative heat transfer occur simultaneously.

Fluidized bed heat transfer phenomena are further complicated due to the large number of significant bed operating parameters which affect transport, among those parameters of importance are bed and heat transfer surface temperatures ; particle size, shape and physical properties ; type of distributor ; fluidizing velocity ; configuration of the immersed surfaces such as size, shape, spacing and pitch ; among others.

A large number of investigations (Alavizadeh, 1985 ; Goshayeshi et al., 1985 ; Lei, 1988 ; Mathur and Saxena, 1987), reported in the literature, have emphasized spatial-averaged heat transfer results. Local, time-averaged heat transfer coefficients for an immersed tube array provide additional information of importance to the fluidized bed combustor designer. A number of recent investigations have reported local heat transfer results. Most of these were restricted to a single tube, and low bed temperatures where tubes were electrically heated and local heat fluxes were evaluated by measuring the power input, along with measurements of tube wall temperatures, for heat transfer coefficient calculations (Goshayeshi et al.,1985).

The objective of the present work is to measure the local bed-to-tube total and radiative heat transfer rates for a horizontal tube array immersed in a high-temperature fluidized bed. Three different bed operating temperatures were employed −705 K, 761 K, and 812 K. Data were obtained for three different particle sizes also. A well-designed instrumented tube capable of measuring both total and radiative heat transfer coefficients between the bed and immersed surfaces, developed by Alavizadeh et al.(1984) and Lei(1988), was employed to evaluate the effect of different bed parameters.

2. Experimental Apparatus

Figure 1 illustrates schematically the instrumented tube used for measuring both total and radiative heat transfer coefficients between the bed and immersed tubes. The instrumented tube, with outside and inside diameters of 51 mm and 32 mm, was made of bronze and equipped with three total and three radiative heat transfer measuring devices. They were mounted side-by-side, each 90 degrees apart, along the axis of the tube.

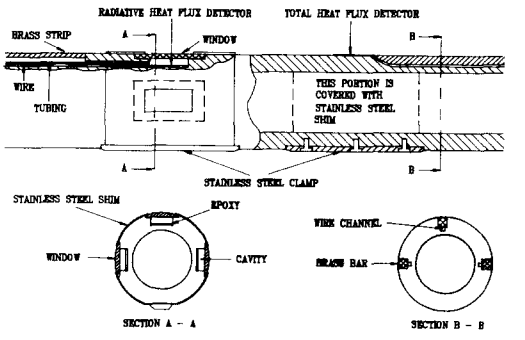

Fig. 1 Instrumented tube for total and radiative heat flux measurements

The micro-foil thermopile-type heat flow detector formed by a thin, low-thermal-conductivity filn with a thermopile on each side was employed as the total and radiative heat flux sensor. Total heat flux sensors were bonded to the tube surface with epoxy and then covered by a 0.127-mm-thick stainless steel shim to protect them from bed abrasion. The shim was pulled tightly over the sensors and connected to the tube with a clamp. A thin film of high-conductivity compound was deposited between the sensors and the shim to reduce thermal contact resistance. Radiation detectors, originally developed by Alavizadeh et al.(1984) and modified by Lei(1988), were used in this work. The radiative component of the total heat transfer from the bed was transmitted through a transparent window mounted on the top of a cavity within the instrumented tube and detected by a heat flux sensor bonded to the base of the cavity. Silicon was employed as the window material and was machined to have the same curvature as the outside of the tube. Silicon has been found to be the superior window material among silicon, sapphire, crystal quartz and fused

quartz as potential candidates for the transmitting window medium (Alavizadeh et al.,1984).

Figure 2 shows a schematic diagram of the experimental equipment. Measurements were conducted in the Oregon State University high-temperature fluidized-bed facility.

Combustion air was compressed and introduced into the system using an air blower. Propane was fed into the burner and burned in a refractory-lined combustion chamber. The hot combustion gases were directed into the 0.3 m × 0.6 m test section through an inconel distributor plate. No combustion occurred in the fluidized-bed itself. A proportional type controller was used to regulate the propane flow rate and maintain the desired gas temperature.

An array of 9 bronze tubes, each with an outside diameter of 51 mm, arranged in three horizontal rows, was used. This staggered arrangement, shown in Fig. 3, is among the most common in-bed tube designs in industrial fluidized-bed combustors (Alavizadeh et al., 1984; Strom et al., 1977; Welty,1983). The instrumented tube was placed in the center of the 9 tubes to represent typical conditions of a tube in an actual large-bed array. The tubes were cooled by circulating water. A rotary union was used to adjust the instrumented tube to desired angular positions for data collection.

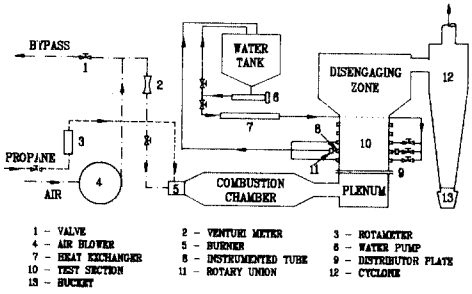

Fig. 2 Schematic of experimental facility

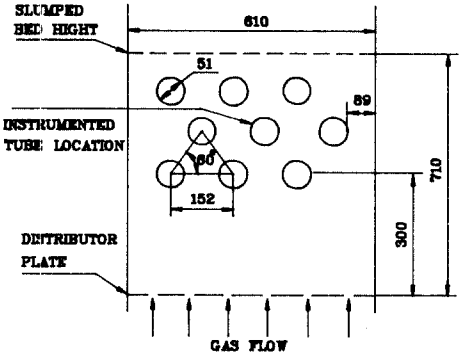

Fig. 3 Tube array geometry

A high-precision digital data acquisition system (HP-3497A) with an HP-85 micro computer connected with an HP-IB interface card and a dual disk drive (HP-83901M), as a control unit, was used to record local heat fluxes and surface temperatures and compute local heat transfer coefficients at each position of the instrumented tube.

3. Experiments

Experiments were conducted at bed tempera-

Table 1 Particle characteristics; size distribution, composition, and properties

Mesh No.	Dpi(mm)	Mass Fraction (%)		
		Sample A	Sample B	Sample C
5~6	3.675	*	*	5.25
6~8	2.855	*	11.19	44.25
8~10	2.180	*	25.36	28.32
10~12	1.850	*	19.11	20.06
12~14	1.550	7.40	9.99	2.22
14~16	1.290	14.72	9.34	*
16~20	1.015	54.27	21.97	*
20~30	0.725	21.20	3.04	*
30~40	0.513	2.41	*	*
Mean Particle Size, $\overline{Dp}$(mm)		0.97	1.53	2.37
Standard Deviation(mm)		0.398	1.035	0.878

Chemical Composition Silica 53.5%, Alumia 43.8%
Titania 2.3%, Other 0.4%

Properties

$\rho_p = 2700$ kg/m^3	
$C_{ps} = 0.853 - 0.982$ kJ/kg.K	(470-900 K)
$k_p = 1.1 - 1.41$ W/mK	(494-833 K)
$\varepsilon_p = 0.855 - 0.874$	(279-452 K)

tures of 705, 761 and 812 K. A granular refractory material (Ione grain) was used as bed material with mean particle diameters of 0.97, 1.53 and 2.37 mm. The mean particle diameter was calculated from the equation suggested by Kunii and Levenspiel(1969). Table 1 shows particle size distribution, chemical composition as given by the supplier and properties (Ghafourian, 1984) of Ione grain.

Data were taken with heat flux sensors positioned at 0, 45, 90, 135 and 180 degrees from the lower stagnation point. Calibration of the heat flux sensor was performed, prior to delivery, by the manufacturer. A calibration to relate the heat flux detected by the radiation sensor to the actual radiation absorbed by the tube wall was carried out locally using a narrow-angle black body source. Details of the calibration techniques and procedures can be found in Alavizadeh(1985) and Alavizadeh et al.(1984).

4. Results and Discussion

All radiative heat transfer coefficients and the radiation contribution in percentage of the total, reported in this study, were calculated for a black tube wall. The values of local total heat transfer coefficient reported in this study are within the range ($+0.08$, -0.14) of actual values, and those of local radiative heat transfer coefficient are within the range ($+0.125$, -0.115) of actual values (Lei, 1988).

Figures 4, 5 and 6 show effects of superficial velocity on the spatial-averaged total and radiative heat transfer coefficients for mean particle diameters 0.97, 1.53 and 2.37 mm at bed temperatures of 705, 761 and 812 K, respectively. For each combination of mean particle diameter and bed temperature, the effect of superficial velocity on spatial-averaged total and radiative heat transfer coefficients was similar. As the superficial velocity, for an initially packed bed, reached the minimum fluidizing velocity (Umf), the spatial-averaged total and radiative heat transfer coefficients increased sharply due to induced particle motion causing replacement of cold particles near the tube wall. As superficial velocities exceeded

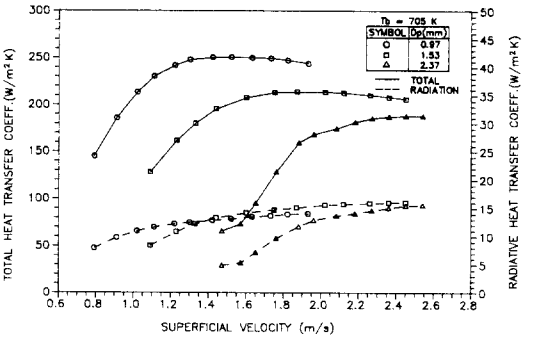

Fig. 4 Total and radiative heat transfer coefficients (spatially averaged) ; bed temperature=705K

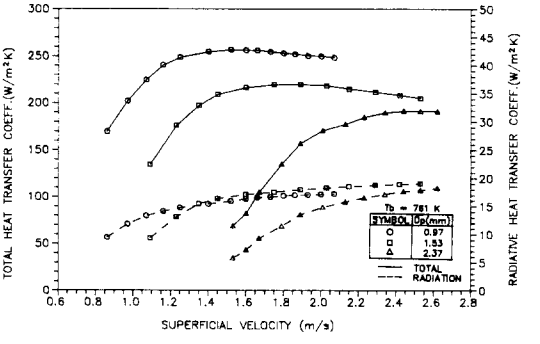

Fig. 5 Total and radiative heat transfer coefficients (spatially averaged) ; bed temperature=761K

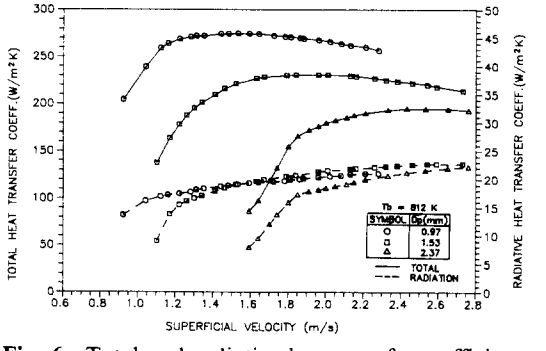

Fig. 6 Total and radiative heat transfer coefficients (spatially averaged) ; bed temperature=812K

Umf, values of the spatial-averaged total heat transfer coefficients increased gradually, reaching maximum values at superficial velocities somewhat greater than the minimum fluidizing velocity, then decreased slowly in all cases for greater values of velocity. This decrease is attributed to a decrease in bed density and greater bubble con-

tact fraction accompanying the increase in superficial velocity. As superficial velocity increased beyond *Umf*, spatial-averaged radiative heat transfer coefficients increased gradually, and appear to approach an asymptotic value. Similar trends have been observed by other investigators (Alavizadeh, 1985; Alavizadeh et al., 1984; Vadivel and Vedamurthy, 1980). Heat transfer rates were always greatest for the smaller particles tested for all test conditions.

Figures 7, 8 and 9 show results of the time-averaged local total heat transfer coefficients around the surface of the tube as functions of superficial velocity for mean particle diameter ($\overline{Dp}$) 0.97 mm and bed temperature (Tb) 705 K; $\overline{Dp}$=1.53 mm and Tb=761 K; and $\overline{Dp}$=2.37 mm and Tb=812 K, respectively. The most obvious effect is the very large change in magnitude of the local total heat transfer coefficient in the region of the upper stagnation point as the superficial velocity was increased. At the lower stagnation point, values of the local total heat transfer coefficient increased with superficial velocity until *Umf* was reached. Values were insensitive to additional changes above the minimum fluidizing velocity.

In Fig. 7, values of local total heat transfer coefficients at the upper stagnation point were observed to increase from 134.2 to 306.6 W/m²K for increases in superficial velocity from 0.79 to 1.93 m/s. At the lower stagnation point, these values increased from 131.0 to 194.5 W/m²K over the same range of superficial velocity.

In general the maximum values of time-averaged local total heat transfer coefficients were at 90 deprees from the lower stagnation point for small superficial velocities, and at the upper stagnation point for higher superficial velocities.

Values of the time-averaged local radiative heat transfer coefficients were at 90 degrees from the lower stagnation point for higher superficial velocities.

Values of the time-averaged local radiative heat transfer coefficients for a representative tube in an array as functions of superficial velocity are displayed in Figs. 10, 11 and 12. Each figure shows results for the same condition as in Figs. 7,

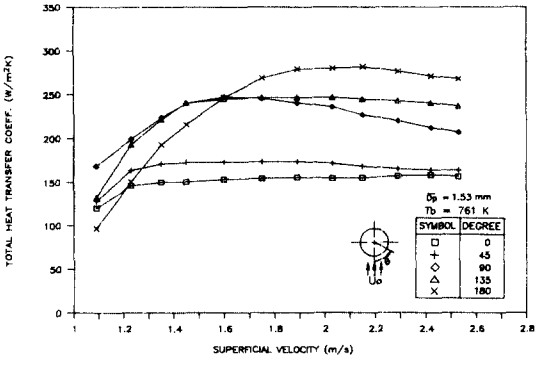

Fig. 8 Local total heat transfer coefficients; mean particle diameter=1.53 mm and bed temperature=761 K

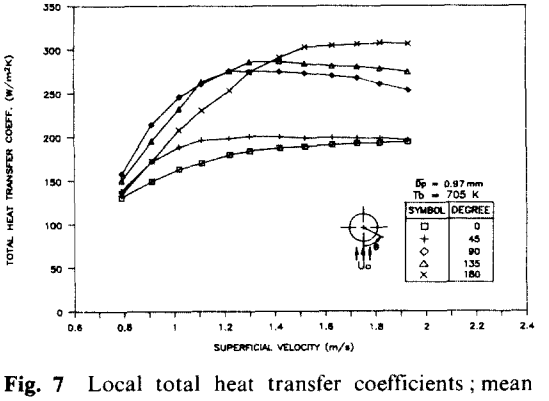

Fig. 7 Local total heat transfer coefficients; mean particle diameter=0.97 mm and bed temperature=705 K

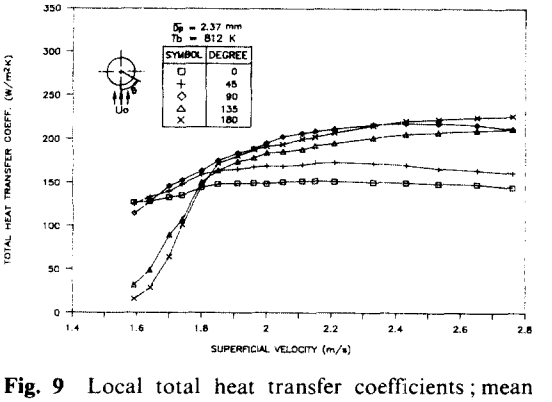

Fig. 9 Local total heat transfer coefficients; mean particle diameter=2.37 mm and bed temperature=812 K

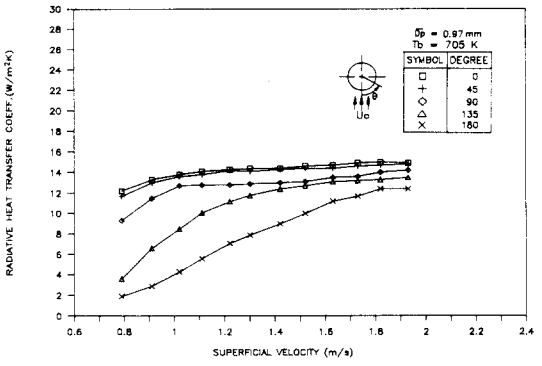

Fig. 10 Local radiative heat transfer coefficients; mean particle diameter=0.97 mm and bed temperature=705 K

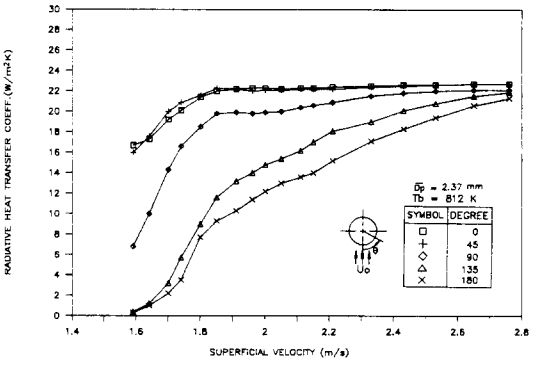

Fig. 12 Local radiative heat transfer coefficients; mean particle diameter=2.37 mm and bed temperature=812 K

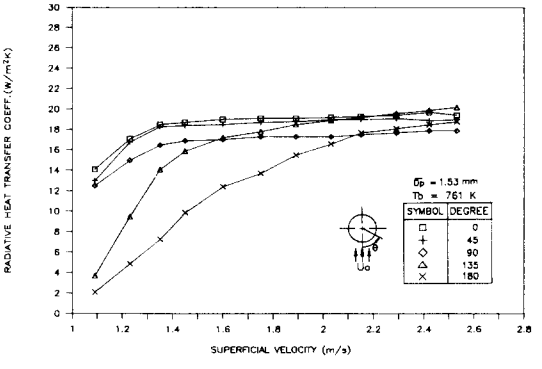

Fig. 11 Local radiative heat transfer coefficients; mean particle diameter=1.53 mm and bed temperature=761 K

8 and 9, respectively. They demonstrate similar tendencies for all particle sizes and bed temperatures. Values of local radiative heat transfer coefficients are relatively low for a packed-bed condition. Local radiative heat transfer coefficients at all locations increased with superficial velocity, the ratio of increase with Uo increasing directly as the distance from the lower stagnation point for all operating conditions. More uniform distributions of local radiative heat transfer coefficients were established for higher values of superficial velocity.

Generally, maximum time-averaged local radiative heat transfer coefficients appeared at the lower stagnation point for all operating conditions.

In the case with a mean particle diameter of 2.37 mm, values of the local radiative heat transfer coefficient at the upper stagnation point increased from 1.0 to 21.3 W/m^{2}K for values of superficial velocity varying from 1.64 to 2.76 m/s; at the lower stagnation point increases between 17.3 and 22.7 W/m^{2}K were measured over this same superficial velocity range.

The low values for local coefficients on the upper half of the tube at low superficial velocities are due to the presence of the relatively cool stagnant defluidized particle cap, the so-called "lee stack". However at velocities above minimum fluidization, the cap was displaced by rising bubbles. Values of local heat transfer coefficients over the lower part of the tube were relatively insensitive to changes in superficial velocity as a result of a gas layer surrounding the lower portion of the tube (Hager and Thomson, 1973; Rowe, 1976).

Figure 13 shows values for the spatial-averaged maximum total heat transfer coefficient and the radiation contribution as functions of mean particle diameter, for bed operating temperatures of 705, 761 and 812 K. In the case with a mean particle diameter of 1.53 mm, maximum values of the heat transfer coefficients increased from 213.8 to 230.8 W/m^{2}K for values of bed temperature varying from 705 to 812 K and radiation contributions increased from 7.07 to 8.99% at these same conditions. Values of the maximum spatial aver-

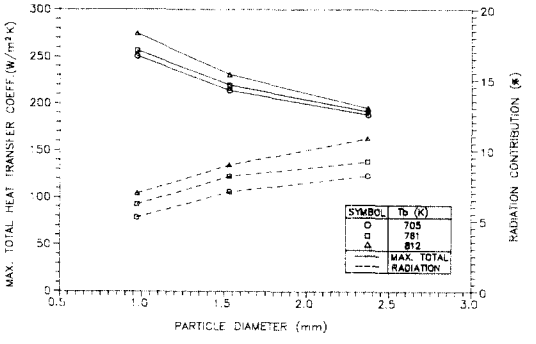

Fig. 13 Maximum total and radiative heat transfer (spatially averaged) as functions of mean particle diameter

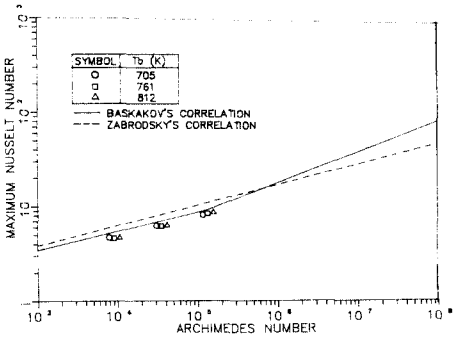

Fig. 14 Maximum Nusselt number variation with Archimedes number

aged heat transfer coefficient decreased and radiation contributions increased with an increase in mean particle size. Even though the radiant contribution was observed to increase with particle size, the maximum heat transfer coefficients decreased with an increase in particle size. This result is in agreement with generally-accepted fluidized bed behavior (Alavizadeh, 1985 ; Lei, 1988).

Figure 14 shows the relationship between the maximum Nusselt number and Archimedes number for the present work. Nusselt numbers and Archimedes numbers were calculated using air properties at operating bed temperatures. Data for the present work agree closely with Baskakov's correlation (Baskakov et al. 1973 a & b), shown in the figure as a solid line.

5. Conclusions

Reported in this paper are experimental values of heat transfer rates, with separate measurements having been made of the radiant contribution for the case of an array of horizontal tubes, immersed in a high temperature fluidized bed. Three different bed operating temperatures were used, these being 705, 761 and 812 K, respectively. Data were obtained for three different sizes of 0.97, 1.53 and 2.37 mm.

Maximum total heat transfer coefficients, spatially averaged around the tube periphery, varied from approximately 275 W/m^2K for highest temperature (812 K) and smallest mean particle size (0.97 mm) to roughly 190 W/m^2K for a bed operating temperature of 705 K and a mean particle diameter of 2.37 mm. Radiation contributions ranged from approximately 11 % for the highest temperature (812 K) and largest mean particle size (2.37 mm) to roughly 5 % for the lowest temperature (705 K) and smallest mean particle diameter (0.97 mm).

Maximum local total heat transfer coefficients appeared at a location 90 degrees from the lower stagnation point for smaller superficial velocities and at the upper stagnation point for higher superficial velocities. Maximum local radiative heat transfer coefficients appeared at the lower stagnation point for all operating conditions.

Relatively good agreement with the correlation of Baskakov(1973 a & b) relating the maximum Nusselt number to the Archimedes number.

Acknowledgment

Appreciation is expressed to Korea Science and Engineering Foundation(KOSEF) whose support provided the means to accomplish this work.

References

Alavizadeh, N., 1985, "An Experimental Investigation of Radiative and Total Heat Transfer Around a Horizontal Tube," Ph.D. Thesis, Dept. of Mech. Eng., Oregon State University.

Alavizadeh, N., Adams, R.L., Welty, J.R. and Goshayeshi, A., 1984, "An Instrument for Local Radiative Heat Transfer Measurement in a Gas Fluidized Bed at Elevated Temperature," New Experimental Techniques in Heat Transfer, The 22nd National Heat Transfer Conf. and Exhibition, ASME HTD-Vol. 31, pp. 1~8.

Baskakov, A.P., Berg, B.A., Vitt, O.K., Filippovsky, N.F., Kirakosyan, V.A., Goldobin, J.M. and Maskaev, V.K., 1973, "Heat Transfer to objects Immersed in Fluidized-Beds," Power Technology, No. 8, pp 273~282.

Baskakov, A.P., Vitt, O.K., Kirakosyan, V.A., Maskaev, V.K. and Filippovsky, N.F., 1973, "Investigation of Heat Transfer Coefficient Pulsations and of the Mechanism of Heat Transfer from a Surface Immersed into a Fluidized Bed," La Fluidisation et Ses Applications-Congress International, Vol. 1, Cepadues, Toulouse, France.

Ghafourian, N.R., 1984, "Determination of Thermal Conductivity, Specific Heat and Emissivity of Ione Grain," MS Project, Dept. of Mech. Eng., Oregon State University.

Goshayeshi, A., Welty, J.R., Adams, R.L. and Alavizadeh, N., 1985, "Local Heat Transfer Coefficients for Horizontal Tube Arrays in High Temperature Large Particle Fluidized Beds.-An Experimental Study," AIChE Symp. Ser. No. 245, Vol. 81, PP. 34~40.

Hager, W.R. and Schrag, S.D., 1976, "Particle Circulation Downstream from a Tube Immersed in a Fluidized Bed," Chem. eng. Sci., Vol. 31, PP. 657~659.

Hager, W.R. and Thomson, W.J., 1973, "Bubble Behavior around Immersed Tubes in a Fluidized Bed," AIChE, Symp. Ser., Vol. 69, No. 128, PP 68~77

Kunii, D. and Levenspiel, O., 1969, "Fluidization engineering," John Wiley & Sons, Inc.

Lei, David Hsien-Yu, 1988, "An Experimental Study of Radiative and Total Heat Transfer between a High Temperature Fluidized Bed and an Array of Immersed Tubes," Ph.D. Thesis, Dept. of Mech. Eng., Oregon State University.

Mathur, A., and Saxena, S.C., 1987, "Total and Radiative Heat Transfer to an Immersed Surface in a Gas-Fluidized Bed," AIChE J., Vol. 33, No. 7, PP. 1124~1135.

Rowe, P.N., 1976, "Prediction of Bubble Size in a Gas Fluidized Bed," Chem. Eng. Sci., Vol. 31, PP. 1081~1091

Strom, S.S., Dowdy, T.E., Lapple, W.C., Kitto, J.B., Stanoch, T.P., Boll, R.H. and Sage, W.L., 1977, "Preliminary Evaluation of Atmospheric Pressure Fluidized Bed Combustion Applied to Electric Utility Large Steam Generators," EPRI Report, No. RP 412-1, Electric Power Research Institute, Palo Alto, CA.

Vadivel, R. and Vedamurthy, V.N., 1980, "An Investigation of the Influence of Bed Parameters on the Variation of the Local Radiative and Total Heat Transfer around an Embedded Horizontal Tube in a Fluidized Bed Combustor," Proc. of 6th Int. Conf. on Fluidized Bed Combustion, Vol. 3, Atlanta, GA. USA.

Welty, J. R., 1983, "Heat Transfer in Large Particle Fluidized Beds," US/CHINA Binational Heat Transfer Workshop, Editors, Z. Wu, B. Wang, C.L. Tien, and K.T. Yang, PP. 148~162.

Zabrodsky, S.S., Antonishin, N.V., Vasiliev, G. M. and Paranas, A.L., 1974, "The Choice of Design Correlation for the Estimation of the High-Temperature Fluidized Bed-to-Immersed Body Heat Transfer Coefficient," Vestn. Akad. Nauk. USSR, Ser, Fiz-Energ. Nauk No. 4, PP. 103~107.